Advances in Applied Mathematics and Mechanics
Adv. Appl. Math. Mech., Vol. **8**, No. 5, pp. 810-826

DOI: 10.4208/aamm.2015.m904
October 2016

Identification of Elastic Orthotropic Material Parameters by the Singular Boundary Method

Bin Chen[1], Wen Chen[1,*] and Xing Wei[2]

[1] *State Key Laboratory of Hydrology-Water Resources and Hydraulic Engineering, College of Mechanics and Materials, Hohai University, Nanjing 210098, China*
[2] *College of Civil Engineering and Architecture, East China Jiaotong University, Nanchang 330013, China*

Received 7 January 2015; Accepted (in revised version) 12 August 2015

Abstract. This article addresses the resolution of the inverse problem for the parameter identification in orthotropic materials with a number of measurements merely on the boundaries. The inverse problem is formulated as an optimization problem of a residual functional which evaluates the differences between the experimental and predicted displacements. The singular boundary method, an integration-free, mathematically simple and boundary-only meshless method, is employed to numerically determine the predicted displacements. The residual functional is minimized by the Levenberg-Marquardt method. Three numerical examples are carried out to illustrate the robustness, efficiency, and accuracy of the proposed scheme. In addition, different levels of noise are added into the boundary conditions to verify the stability of the present methodology.

AMS subject classifications: 62P30, 65M32, 65K05

Key words: Inverse problems, parameter identification, meshless method, singular boundary method, Levenberg-Marquardt method.

1 Introduction

Elastic constants are routinely obtained from laboratory tests on the specimens with a well-defined standardized geometry and loading. A uniaxial stress test is used to identify one or two material properties. Thus for orthotropic materials, such as wood, many crystals, and rolled metals, more mechanical tests along the orthogonal principal axes of the material are required to determine all the mechanical properties. Moreover, in some cases the mechanical property of materials may be changed due to the manufacturing

*Corresponding author.
Email: chenwen@hhu.edu.cn (W. Chen)

 ©2016 Global Science Press

https://doi.org/10.4208/aamm.2015.m904 Published online by Cambridge University Press

conditions, and the test samples are not available [1–3]. As a consequence, the mixed numerical-experimental techniques are developed.

Thanks to the development of experimental devices and numerical methodologies in the past decades, the mixed numerical-experimental techniques have been successfully applied in the parameter identification problem [4–6]. Mixed numerical-experimental techniques, namely inverse methods, are based on static loading experiments, optimization techniques, full-field measurement techniques, and numerical modeling. The aim of the inverse methods is to identify the mechanical properties with a reduced experimental set-up. The advantage of the inverse methods lies in that non-standardized specimen geometries as well as more complicated boundary conditions and material models can be taken into consideration. For these reasons, the inverse methods are attractive to extract constitutive parameters from the stress/strain/displacement fields, either for composites or for other materials [7–9].

Quite a few numerical techniques are developed to solve the parameter identification problems, such as the constitutive equation gap method (CEGM) [10, 11], finite element method (FEM) [12–15], virtual fields method (VFM) [16–19], and boundary element method (BEM) [3, 20–22]. The basic idea of the VFM is to apply the principle of virtual work to the tested specimen with some explicit and independent virtual displacement fields. Each virtual field provides a linear equation based on the principle of virtual work and finally leads to a linear system to directly determine the unknown parameters. However, the specimen geometry must be defined to balance the influences of each unknown parameter and a set of available virtual fields leading to a well-conditioned system are required in the VFM. In the other methods, the parameter identification problem is formulated as an optimization problem of a least square residual functional which evaluates the differences between the experimental and predicted displacements. The numerical methods are only involved in the solution of the direct problems to obtain the predicted displacements with estimated parameters. The least square residual functional is minimized by an optimization method, i.e., Levenberg-Marquardt method in this study.

Among the numerical methods, the FEM requires mesh generation and re-meshing which is computationally expensive and sometimes mathematically troublesome, especially for the complex specimen. In addition, the FEM encounters the difficulties of raising the regularity of the approximation. The CEGM stems from a more general approach developed for updating FEM models from assessing quality of FEM meshes or vibration data. Up to now, another three techniques based on FEM models have been widely employed: the reciprocity gap method [23], the equilibrium gap method [24, 25], and multistep reciprocity gap function method [26]. A good survey of these techniques can be found in [27] with a focus on noisy data in [28]. By contrast, the BEM requires only meshing on the boundary. But nevertheless the BEM involves sophisticated mathematics and numerical integrations due to singular fundamental solutions. To avoid these difficulties, the method of fundamental solutions (MFS) [29, 30] approximates the solution with a linear combination of fundamental solutions with respect to the source points in

https://doi.org/10.4208/aamm.2015.m904 Published online by Cambridge University Press

the strong-form collocation fashion and regularizes the source singularity of fundamental solutions by placing an auxiliary boundary outside the physical domain. However, the location of the auxiliary boundary is a perplexing and controversial issue, especially in practical problems with complex-shaped or multi-connected domains. Inspired by the BEM, a recent boundary only collocation method the singular boundary method (SBM) [31–37], introduces the origin intensity factor to isolate the singularities of the fundamental solutions so that the source points could be directly collocated on the physical boundary. This method is mathematically simple, easy to program, and truly free of mesh and integration. These salient advantages of the SBM have been further demonstrated by some recent developments [32–37]. In this study, we document the application of the SBM in the identification of elastic parameters for orthotropic materials.

The rest of the paper is organized as follows. In Section 2, we establish the SBM formulation for the elastic analysis problem of orthotropic materials. The inverse analysis based on the SBM is introduced in Section 3. And then in Section 4 the proposed scheme is tested over some benchmark cases. Finally, Section 5 draws the conclusions upon the numerical experiments.

2 The singular boundary method for two-dimensional orthotropic material bodies

2.1 Governing equations and fundamental solutions

The general stress-strain relation of the two-dimensional orthotropic composites can be given by

$$\begin{Bmatrix} \varepsilon_{11} \\ \varepsilon_{22} \\ \gamma_{12} \end{Bmatrix} = \begin{bmatrix} s_{11} & s_{12} & 0 \\ s_{21} & s_{22} & 0 \\ 0 & 0 & s_{66} \end{bmatrix} \begin{Bmatrix} \sigma_{11} \\ \sigma_{22} \\ \tau_{12} \end{Bmatrix}, \tag{2.1}$$

where ε_{11}, ε_{22} and γ_{12} are strain components, σ_{11}, σ_{22} and τ_{12} stress components, s_{11}, s_{12}, s_{21}, s_{22} and s_{66} compliance components. Only four of the five compliance components are independent since $s_{12}=s_{21}$.

Employing the equilibrium equations and the general stress-strain relation (2.1), the Navier-Cauchy equations for two-dimensional elastic orthotropic material bodies, in the absence of body forces, can be stated as

$$C_{11}\frac{\partial^2 u_1(x)}{\partial x_1^2}+(C_{12}+C_{66})\frac{\partial^2 u_2(x)}{\partial x_1 \partial x_2}+C_{66}\frac{\partial^2 u_1(x)}{\partial x_2^2}=0, \tag{2.2a}$$

$$C_{22}\frac{\partial^2 u_2(x)}{\partial x_1^2}+(C_{12}+C_{66})\frac{\partial^2 u_1(x)}{\partial x_1 \partial x_2}+C_{66}\frac{\partial^2 u_2(x)}{\partial x_2^2}=0, \tag{2.2b}$$

where u_1 and u_2 represent the horizontal displacement and the vertical displacement, respectively, $C_{11}=s_{22}/D$, $C_{12}=-s_{12}/D$, $C_{22}=s_{11}/D$, $C_{11}=1/s_{66}$, $D=s_{11}s_{22}-s_{12}^2$. The

https://doi.org/10.4208/aamm.2015.m904 Published online by Cambridge University Press

following boundary conditions are subjected to the boundary

$$u_i(x)=\bar{u}_i,\quad x\in\Gamma_u\quad\text{and}\quad t_i(x)=\bar{t}_i,\quad x\in\Gamma_t,\quad i=1,2, \tag{2.3}$$

where Γ_u and Γ_t construct the whole boundary of the physical domain, $t_i(x)$ and $u_i(x)$ denote the component of boundary traction and displacement in the ith coordinate direction, $\bar{u}_i$ and $\bar{t}_i$ represent the prescribed displacements and tractions, respectively.

For plane orthotropic materials, the fundamental solutions for Eqs. (2.1) and (2.2) can be expressed as [38]

$$u_{11}(x,y)=K\big(\alpha_1^{\frac{1}{2}}A_2^2\log r_1-\alpha_2^{\frac{1}{2}}A_1^2\log r_2\big), \tag{2.4a}$$

$$u_{12}(x,y)=-KA_1A_2\Big(\arctan\Big(\alpha_1^{-\frac{1}{2}}\frac{x_2-y_2}{x_1-y_1}\Big)-\arctan\Big(\alpha_2^{-\frac{1}{2}}\frac{x_2-y_2}{x_1-y_1}\Big)\Big), \tag{2.4b}$$

$$u_{21}(x,y)=u_{12}(x,y), \tag{2.4c}$$

$$u_{22}(x,y)=K\big(A_2^2\log r_2\alpha_2^{-\frac{1}{2}}-A_1^2\log r_1\alpha_1^{-\frac{1}{2}}\big), \tag{2.4d}$$

in which y denotes the source point located on the physical boundary, α_1 and α_2 satisfy

$$\alpha_1+\alpha_2=(2s_{12}+s_{66})/(s_{22}),\quad \alpha_1\alpha_2=s_{11}/s_{22},$$

and

$$r_i=\sqrt{\alpha_i(x_1-y_1)^2+(x_2-y_2)^2},\quad A_i=s_{12}-\alpha_i s_{22},\quad K=(2\pi(\alpha_1-\alpha_2)s_{22})^{-1}.$$

The fundamental solutions for the tractions are obtained by deriving the fundamental solutions for the strains and then applying general stress-strain relation (2.1)

$$t_{11}(x,y)=-K\Big(((x_1-y_1)n_1(x)+(x_2-y_2)n_2(x))\Big(\frac{A_1}{r_2^2}\alpha_2^{\frac{1}{2}}-\frac{A_2}{r_1^2}\alpha_1^{\frac{1}{2}}\Big)\Big), \tag{2.5a}$$

$$\begin{aligned}t_{12}(x,y)=&-K\frac{A_2}{r_2^2}(\alpha_2^{\frac{1}{2}}(x_1-y_1)n_2(x)-\alpha_2^{-\frac{1}{2}}(x_2-y_2)n_1(x))\\&+K\frac{A_1}{r_1^2}(\alpha_1^{\frac{1}{2}}(x_1-y_1)n_2(x)-\alpha_1^{-\frac{1}{2}}(x_2-y_2)n_1(x)),\end{aligned} \tag{2.5b}$$

$$\begin{aligned}t_{21}(x,y)=&-K\frac{A_1\alpha_2}{r_2^2}(\alpha_2^{\frac{1}{2}}(x_1-y_1)n_2(x)-\alpha_2^{-\frac{1}{2}}(x_2-y_2)n_1(x))\\&+K\frac{A_2\alpha_1}{r_1^2}(\alpha_1^{\frac{1}{2}}(x_1-y_1)n_2(x)-\alpha_1^{-\frac{1}{2}}(x_2-y_2)n_1(x)),\end{aligned} \tag{2.5c}$$

$$t_{22}(x,y)=-K\Big(((x_1-y_1)n_1(x)+(x_2-y_2)n_2(x))\Big(\frac{A_2}{r_2^2}\alpha_2^{\frac{1}{2}}-\frac{A_1}{r_1^2}\alpha_1^{\frac{1}{2}}\Big)\Big), \tag{2.5d}$$

where $n_i(x)$ is the ith-direction cosine of the unit outward normal vector to the point x.

https://doi.org/10.4208/aamm.2015.m904 Published online by Cambridge University Press

2.2 Singular boundary method

In the SBM formulation, the displacements and tractions are approximated by a linear combination of fundamental solutions with respect to source points y^n as follows:

$$u_i(x^m)=\sum_{n=1}^{N}\alpha_j(y^n)u_{ij}(x^m,y^n), \tag{2.6a}$$

$$t_i(x^m)=\sum_{n=1}^{N}\alpha_j(y^n)t_{ij}(x^m,y^n), \tag{2.6b}$$

where $i,j=1,2,\cdots,N$, is the specified number of the source points, x^m and y^n denote the mth collocation point and nth source point on the physical boundary, and $\alpha_j(y^n)$ means the unknown coefficients. It should be stressed that the collocation and source points coincide and are placed on the physical boundary in the SBM. Therefore, the fundamental solutions $u_{ij}(x^m,y^n)$ and $t_{ij}(x^m,y^n)$ are singular when the collocation point x^m overlaps the source point y^n. To isolate the singularity of the fundamental solutions, the SBM introduces a concept of the origin intensity factor. With the employment of the origin intensity factor, the SBM solution of the displacements and tractions are recast as

$$u_i(x^m)=\sum_{n=1,\ m\neq n}^{N}\alpha_j(y^n)u_{ij}(x^m,y^n)+\alpha_j(y^m)A_{ij}(y^m), \tag{2.7a}$$

$$t_i(x^m)=\sum_{n=1,\ m\neq n}^{N}\alpha_j(y^n)t_{ij}(x^m,y^n)+\alpha_j(y^m)B_{ij}(y^m), \tag{2.7b}$$

where $A_{ij}(y^m)$ and $B_{ij}(y^m)$ are defined as the origin intensity factors. The strategy for the evaluation of the origin intensity factors can be found in [35], namely

$$B_{ij}(y^m)=\frac{1}{L_m}\Big[\delta_{ij}+I_m+\sum_{n=1,\ n\neq m}^{N}t_{ij}(y^n,x^m)L_n\Big], \tag{2.8}$$

where $I_m=\int_{\Gamma_m}[t_{ij}(x^m,y)+t_{ij}(y,x^m)]d\Gamma_m$ approximated by the Trapezoidal quadrature formula, L_n denotes the half distance between the $(n-1)$th and $(n+1)$th nodes. It can be observed that the origin intensity factor A_{ij} contains the singular term $\log r_i$. The origin intensity factors a_{mm} of $\log r$ can be easily calculated via $a_{mm}=\log\frac{L_m}{2\pi}$ [36, 37]. Then the origin intensity factors a_{mmi} of $\log r_i$ can be obtained via coordinate transform. Finally A_{ij} can be determined as follows

$$A_{11}(y^m)=K\big(\alpha_1^{\frac{1}{2}}A_2^2a_{mm1}-\alpha_2^{\frac{1}{2}}A_1^2a_{mm2}\big), \tag{2.9a}$$

$$A_{12}(y^m)=-KA_1A_2\Big(\arctan\Big(\frac{n_2(y^m)}{\alpha_1n_1(y^m)}\Big)-\arctan\Big(\frac{n_2(y^m)}{\alpha_2n_1(y^m)}\Big)\Big), \tag{2.9b}$$

$$A_{21}(y^m)=A_{12}(y^m), \tag{2.9c}$$

$$A_{22}(y^m)=K\big(A_2^2a_{mm2}\alpha_2^{-\frac{1}{2}}-A_1^2a_{mm1}\alpha_1^{-\frac{1}{2}}\big). \tag{2.9d}$$

https://doi.org/10.4208/aamm.2015.m904 Published online by Cambridge University Press

With the computing origin intensity factors, we obtain D_{ij} as below

$$D_{ij}=\begin{bmatrix} A_{ij}(x^1) & u_{ij}(x^1,y^2) & \cdots & u_{ij}(x^1,y^{N_1}) \\ u_{ij}(x^2,y^1) & A_{ij}(x^2) & \cdots & u_{ij}(x^2,y^{N_1}) \\ \vdots & \vdots & \ddots & \vdots \\ u_{ij}(x^{N_1},y^1) & u_{ij}(x^{N_1},y^2) & \cdots & A_{ij}(x^{N_1}) \\ t_{ij}(x^{N_1+1},y^1) & t_{ij}(x^{N_1+1},y^2) & \cdots & t_{ij}(x^{N_1+1},y^{N_1}) \\ t_{ij}(x^{N_1+2},y^1) & t_{ij}(x^{N_1+2},y^2) & \cdots & t_{ij}(x^{N_1+2},y^{N_1}) \\ \vdots & \vdots & \ddots & \vdots \\ t_{ij}(x^{N_1},y^1) & t_{ij}(x^N,y^2) & \cdots & t_{ij}(x^N,y^{N_1}) \end{bmatrix}$$
$$\begin{bmatrix} u_{ij}(x^1,y^{N_1+1}) & u_{ij}(x^1,y^{N_1+2}) & \cdots & u_{ij}(x^1,y^N) \\ u_{ij}(x^2,y^{N_1+1}) & u_{ij}(x^2,y^{N_1+2}) & \cdots & u_{ij}(x^2,y^N) \\ \vdots & \vdots & \ddots & \vdots \\ u_{ij}(x^{N_1},y^{N_1+1}) & u_{ij}(x^{N_1},y^{N_1+2}) & \cdots & u_{ij}(x^{N_1},y^N) \\ B_{ij}(x^{N_1+1}) & t_{ij}(x^{N_1+1},y^{N_{1+2}}) & \cdots & t_{ij}(x^{N_1+1},y^N) \\ t_{ij}(x^{N_1+2},y^{N_1+1}) & B_{ij}(x^{N_1+2}) & \cdots & t_{ij}(x^{N_1+2},y^N) \\ \vdots & \vdots & \ddots & \vdots \\ t_{ij}(x^N,y^{N_1+1}) & t_{ij}(x^N,y^{N_1+2}) & \cdots & B_{ij}(x^N) \end{bmatrix}. \tag{2.10}$$

Then we can obtain the following linear equations to determine the unknown coefficients by the collocation method

$$\mathbf{D}\alpha=\mathbf{b}, \tag{2.11}$$

where

$$D=\begin{bmatrix} D_{11} & D_{12} \\ D_{21} & D_{22} \end{bmatrix}$$

is the coefficient matrix, α the unknown density vector, and b the right-hand side vector. Finally mechanical responses of whole domain are obtained by using Eqs. (2.6a) and (2.6b).

3 Inverse analysis based on the singular boundary method

3.1 Objective function

In the parameter identification problem, the compliance components in the constitutive relations, i.e., s_{11}, s_{22}, s_{12}, s_{66}, are unknown. With boundary data measured by the experimental technique, the parameter identification process can be formulated as an optimization problem. The objective function is defined as a square sum of differences between

https://doi.org/10.4208/aamm.2015.m904 Published online by Cambridge University Press

the measured and numerically determined displacements:

$$F(s)=\frac{1}{2}\sum_{i=1}^{p}(u_i(s)-u_i^*)^2,\quad s\in R^q,\quad p\geq q, \tag{3.1}$$

where the vector $s_T=[s_{11},s_{22},s_{12},s_{66}]$, p is the number of the measured displacements, q is the number of the parameters to be determined, $u_i(s)$ and u_i^* denote the calculated displacement by the SBM and the measured displacement, respectively. In order to account for the aleatoric uncertainties in the measurements, different levels of noise are added into the actual displacement by

$$u_i^*=(1+\delta\cdot\zeta)u_i^e, \tag{3.2}$$

where u_i^e represents the actual displacement, δ the guess maximum positive relative error of the measured displacement, ζ a Gaussian random variable with zero mean and unit standard deviation. Unless otherwise specified, the default setting of δ equals to zero.

3.2 Levenberg-Marquardt method

It is recommended in literature that gradient-based methods are more preferable if accurate derivative information can be computed efficiently and globally. The SBM formulation provides convenience for direct differentiation. Thus, the Levenberg-Marquardt (LM) method [39] is introduced to minimize the objective function in Eq. (3.1). The LM method can be viewed as the Gauss-Newton method modified by the model trust region approach and avoid the poor performance of the Gauss-Newton method when the Jacobian matrix is rank-deficient [40]. In addition, the LM method is more robust and can find a solution even if the initial guess is far away from the final minimum.

The gradient of the objective function can be described by

$$\nabla F(s)=\frac{\partial F(s)}{\partial s_j}=\sum_{i=1}^{p}\Big(\frac{\partial u_i(s)}{\partial s_j}\Big)(u_i(s)-u_i^*), \tag{3.3}$$

where the partial derivatives of the displacement with respect to the parameter values, $\partial u_i(s)/\partial s_j$, are the sensitivity coefficients. Based on the sensitivity coefficients, the Jacobian matrix $J(s)$ can be obtained by

$$J(s)=\begin{bmatrix}\dfrac{\partial u_1(s)}{\partial s_1} & \dfrac{\partial u_1(s)}{\partial s_2} & \cdots & \dfrac{\partial u_1(s)}{\partial s_q}\\ \dfrac{\partial u_2(s)}{\partial s_1} & \dfrac{\partial u_2(s)}{\partial s_2} & \cdots & \dfrac{\partial u_2(s)}{\partial s_q}\\ \vdots & \vdots & \ddots & \vdots\\ \dfrac{\partial u_p(s)}{\partial s_1} & \dfrac{\partial u_p(s)}{\partial s_2} & \cdots & \dfrac{\partial u_p(s)}{\partial s_q}\end{bmatrix}. \tag{3.4}$$

https://doi.org/10.4208/aamm.2015.m904 Published online by Cambridge University Press

The calculation of Jacobian matrix is based on the calculated displacements by the SBM. With an initial feasible guess of s, the LM method updates the parameters until the specified criteria are achieved. The parameters at iteration k are updated via the following equations

$$\left[J(s^{(k)})^T J(s^{(k)})+\mu^{(k)} I\right]\delta^{(k)} = -J(s^{(k)})^T (u(s^{(k)})-u^*), \tag{3.5a}$$

$$s^{(k+1)} = s^{(k)}+\delta^{(k)}, \tag{3.5b}$$

where $\mu^{(k)}$ is a positive scalar named Levenberg-Marquardt parameter, and I the identity matrix. The convergence criteria are defined as

$$\left\|J(s^{(k)})^T (u(s^{(k)})-u^*)\right\| < \varepsilon_1 \quad \text{and} \quad \sum_{i=1}^{q}\left|\frac{s_i^{(k+1)}-s_i^{(k)}}{s_i^{(k)}}\right| < \varepsilon_2, \tag{3.6}$$

where ε_1 and ε_2 are the specified accuracy requirements.

3.3 Solution algorithm

The main idea of the present algorithm relies on applying the SBM combined with the LM method. The procedure described above may be summarized as follows:

Step 1 Give an initial guess s_0 of the undetermined parameters and form a direct problem.

Step 2 Solve the direct problem to obtain the unknown density vector α in Eq. (2.11).

Step 3 Calculate the displacement $u_i(s)$ by the SBM and achieve the objective function $F(s)$.

Step 4 Minimize the objective function $F(s)$ through the LM method and meanwhile update the undetermined parameters.

Step 5 Form a new direct problem with the updated parameters and then switch to Steps 2-4. Finally obtain the identified parameters when the convergence criteria are achieved.

4 Numerical examples

The following examples illustrate the validity of the proposed scheme. For each example, the actual material parameters of orthotropic material [41] and their bounds are listed in Table 1. The displacements derived from the SBM with the actual material parameters are taken as the measured ones in the parameter identification process. Unless otherwise specified, the initial Levenberg-Marquardt parameter is taken as $\mu^{(0)} = 1e^{-12}$. The stopping criteria are $\varepsilon_1 = 10^{-6}$ and $\varepsilon_2 = 10^{-3}$ for Eq. (3.5b).

https://doi.org/10.4208/aamm.2015.m904 Published online by Cambridge University Press

Table 1: The true values of material parameters and their bounds.

Parameter	True value (10^{-10}Pa^{-1})	Lower bound (10^{-10}Pa^{-1})	Upper bound (10^{-10}Pa^{-1})
s_{11}	0.068074	0.015000	0.350000
s_{22}	0.918270	0.200000	4.500000
s_{12}	-0.025968	-0.100000	-0.005000
s_{66}	1.560100	0.300000	7.500000

Example 4.1. As shown in Fig. 1, a rectangular orthotropic plate (100mm$\times$50mm) subjected to a uniform tension of 20MPa on the right side is investigated. The horizontal boundaries (upper and lower) are discretized into 20 boundary nodes, whereas the vertical ones (left and right) into 10 boundary nodes each, as shown in Fig. 2. We assume the elastic parameters s_{22} and s_{66} are prior specified and thus only need to identify s_{11} and s_{12}. Vertical displacements at nodes $21(-20,50)$ and $30(20,50)$ and horizontal displacements at node $26(0,50)$ are the measured data.

To illustrate the efficiency of the LM method, the Quasi Newton (QN) method [42] and pattern search (PS) method [43] are also used for comparison. Four different initial guesses are considered in this example, and the identified results are listed in Table 2. It is observed that all three methods achieve satisfactory results. The LM method and the PS method converge to actual values within 4 iterations, while the QN method requires more iterations. The reason lies in that the QN method converges slowly towards to the optimum in comparison with the LM method and PS method. On the other side,

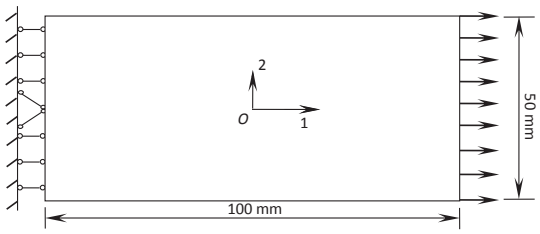


Figure 1: A rectangular orthotropic plate.

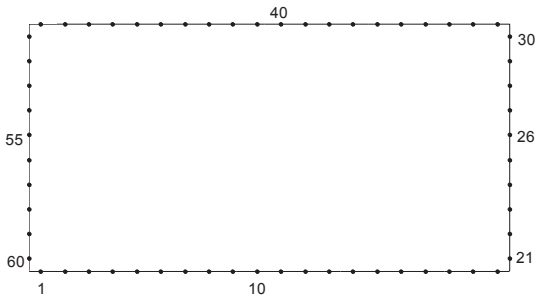


Figure 2: Boundary collocation points of the rectangular plate.

https://doi.org/10.4208/aamm.2015.m904 Published online by Cambridge University Press

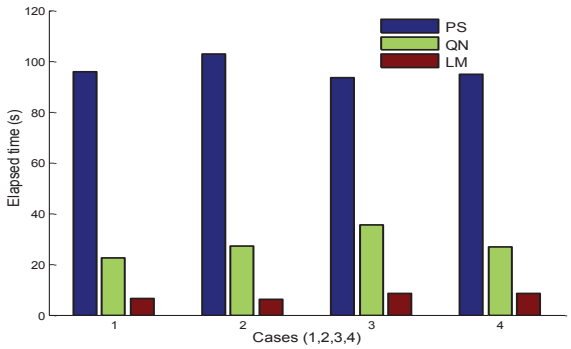


Figure 3: Elapsed time of three methods in different cases.

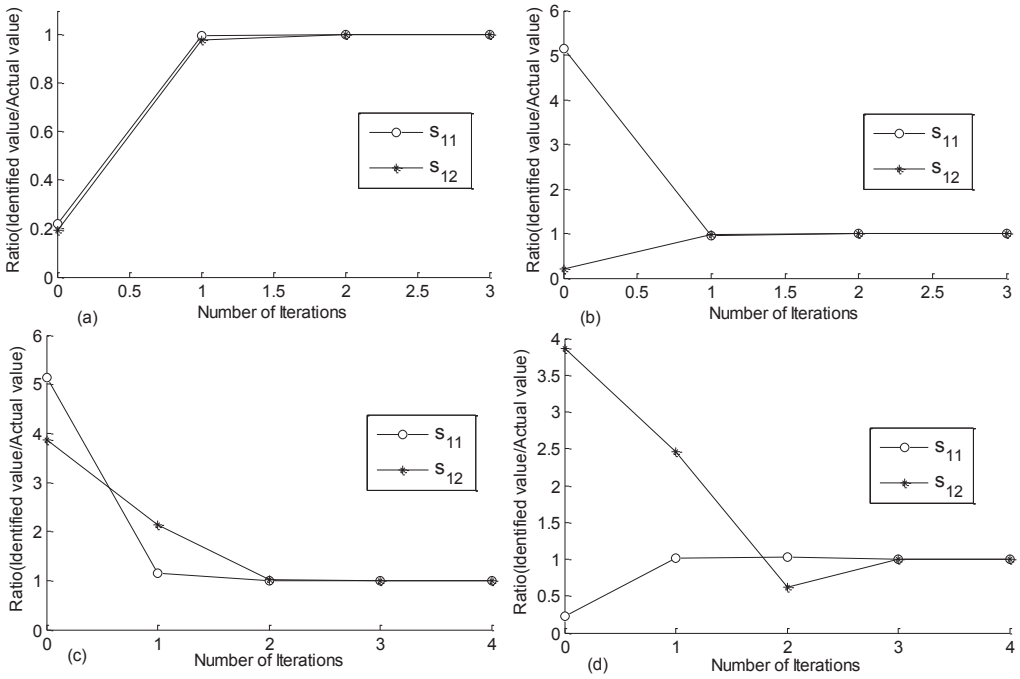


Figure 4: Identification process of the parameters s_{11} and s_{12} with the LM method: (a) Case 1; (b) Case 2; (c) Case 3; (d) Case 4.

the PS method searches the optimum in a stencil-based fashion with a set of directions. Therefore, much more objective function evaluations are involved. For these reasons, the LM method consumes the least CPU time on searching these results in four different cases, as shown in Fig. 3. Particularly, Fig. 4 displays the identification process of the LM method.

From the above comparisons, it is observed that the LM method is more efficient in the inverse identification problem. Thus, the LM method is selected in the following cases.

https://doi.org/10.4208/aamm.2015.m904 Published online by Cambridge University Press

Table 2: Identified parameters (s_{11},s_{12}) of the rectangular orthotropic plate.

Cases	Parameters ($\times 10^{-10}$Pa^{-1})	Initial values	True values	Identified			Iterations		
				LM	QN	PS	LM	QN	PS
1	s_{11}	0.015	0.068074	0.068078	0.067667	0.068076	3	6	4
	s_{12}	-0.005	-0.025868	-0.025869	-0.028394	-0.025865			
2	s_{11}	0.350	0.068074	0.068077	0.068002	0.068078	3	7	4
	s_{12}	-0.005	-0.025868	-0.025867	-0.025782	-0.025871			
3	s_{11}	0.350	0.068074	0.068077	0.068002	0.068070	4	8	4
	s_{12}	-0.100	-0.025868	-0.025867	-0.025791	-0.025885			
4	s_{11}	0.015	0.068074	0.068077	0.680101	0.068076	4	7	4
	s_{12}	-0.100	-0.025868	-0.025868	-0.025807	-0.025869			

Example 4.2. A 50mm $\times$ 50mm square orthotropic plate is considered under uniform tension and tangential force as shown in Fig. 5. To guarantee the uniqueness of the displacement field, the rigid body motion should be prevented. Thus the three displacement constraints are imposed as boundary conditions: the 1-direction and 2-direction displacements at the point $(-25,-25)$ and the 1-direction displacement at the point $(-25,25)$. Each boundary is divided into 10 boundary nodes, as shown in Fig. 6.

Different from the previous example, all four independent compliance components $(s_{11},s_{12},s_{22}$ and $s_{66})$ are identified. Vertical and horizontal displacements at nodes

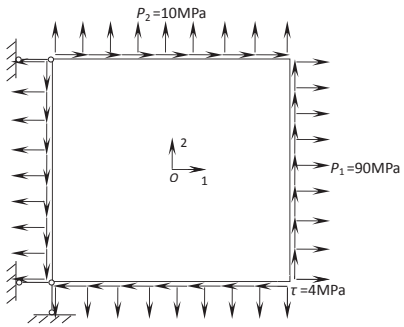


Figure 5: A square orthotropic plate.

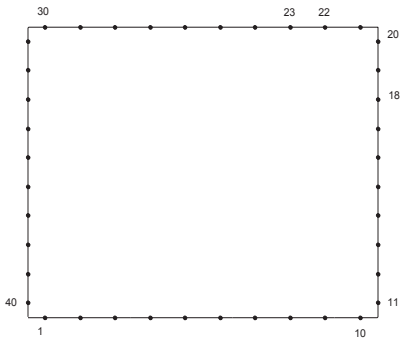


Figure 6: Boundary collocation points of the square plate.

https://doi.org/10.4208/aamm.2015.m904 Published online by Cambridge University Press

Table 3: Identified parameters $(s_{11},s_{12},s_{22},s_{66})$ of the square orthotropic plate.

Cases	Parameters ($\times 10^{-10}$Pa^{-1})	Initial values	True values	Initial/True	Identified	Iterations
1	s_{11}	0.015	0.068074	0.22	0.068074	4
	s_{12}	-0.008	-0.025868	0.31	-0.025868	
	s_{22}	0.250	0.918270	0.27	0.918270	
	s_{66}	0.450	1.560100	0.29	1.560100	
2	s_{11}	0.015	0.068074	0.22	0.068074	6
	s_{12}	-0.008	-0.025868	0.31	-0.025868	
	s_{22}	3.000	0.918270	3.27	0.918270	
	s_{66}	0.450	1.560100	0.29	1.560100	
3	s_{11}	0.0150	0.068074	0.22	0.068074	6
	s_{12}	-0.008	-0.025868	0.31	-0.025868	
	s_{22}	3.000	0.918270	3.27	0.918270	
	s_{66}	5.500	1.560100	3.53	1.560100	
4	s_{11}	0.300	0.068074	4.41	0.068074	4
	s_{12}	-0.008	-0.025868	0.31	-0.025868	
	s_{22}	3.000	0.918270	3.27	0.918270	
	s_{66}	5.500	1.560100	3.53	1.560100	
5	s_{11}	0.300	0.068074	4.41	0.068074	4
	s_{12}	-0.100	-0.025868	3.87	-0.025868	
	s_{22}	3.000	0.918270	3.27	0.918270	
	s_{66}	5.500	1.560100	3.53	1.560100	
6	s_{11}	0.025	0.068074	0.38	0.068074	5
	s_{12}	-0.075	-0.025868	2.9	-0.025868	
	s_{22}	0.250	0.918270	0.23	0.918270	
	s_{66}	5.500	1.560100	3.53	1.560100	

18(25,12.5), 20(25,22.5), 22(17.5,25), and 23(12.5,25) are the measured data during the identification process. The results are tabulated in Table 3. The identified material parameters agree well with the real material parameters, even if the initial guesses deviate dramatically from the actual parameters. Furthermore, in order to take the aleatoric uncertainties of the measurements into account, different levels of noise are added into boundary conditions. Table 4 and Table 5 present the results with noisy boundary conditions. The relative noise level δ varying from 1% to 7% is involved in the calculation. As δ increases, the present method also performs consistently well. Nevertheless, more iterations are required to achieve the stopping criteria.

Example 4.3. This example is concerned with a non-standard multiple connected plate. The geometrical configuration and boundary conditions are shown in Fig. 7. $r=10$mm, $a=40$mm, $P=10$MPa are set up and s_{66} is assumed to be known. Each boundary of the square is discretized into 20 boundary nodes, and the boundary of the inner circle is discretized into 40 nodes. The horizontal displacements at nodes (20,10), (20,20), (20,30) and vertical displacements at nodes $(-20,10)$, $(-20,20)$, $(-20,30)$ are taken as the additional measurements.

Four different cases are studied and the identified results are shown in Table 6. It is observed that satisfactory results are obtained albeit non-standardized domains. Nevertheless, more iterations are required than in the previous two examples. This indicates

https://doi.org/10.4208/aamm.2015.m904 Published online by Cambridge University Press

Table 4: Identified parameters $(s_{11},s_{12},s_{22},s_{66})$ of the square orthotropic plate by considering $\delta=1\%$.

Cases	Parameters ($\times10^{-10}$Pa^{-1})	Initial values	True values	Initial/True	Identified	Iterations
1	s_{11}	0.015	0.068074	0.22	0.067869	3
	s_{12}	-0.008	-0.025868	0.31	-0.024997	
	s_{22}	0.250	0.918270	0.27	0.90858	
	s_{66}	0.450	1.560100	0.29	1.561672	
2	s_{11}	0.015	0.068074	0.22	0.068681	5
	s_{12}	-0.008	-0.025868	0.31	-0.028087	
	s_{22}	3.000	0.918270	3.27	0.934534	
	s_{66}	0.450	1.560100	0.29	1.555285	
3	s_{11}	0.0150	0.068074	0.22	0.068037	4
	s_{12}	-0.008	-0.025868	0.31	-0.023398	
	s_{22}	3.000	0.918270	3.27	0.898556	
	s_{66}	5.500	1.560100	3.53	1.559253	
4	s_{11}	0.300	0.068074	4.41	0.067845	3
	s_{12}	-0.008	-0.025868	0.31	-0.023464	
	s_{22}	3.000	0.918270	3.27	0.890181	
	s_{66}	5.500	1.560100	3.53	1.565675	
5	s_{11}	0.300	0.068074	4.41	0.068504	3
	s_{12}	-0.100	-0.025868	3.87	-0.026544	
	s_{22}	3.000	0.918270	3.27	0.919959	
	s_{66}	5.500	1.560100	3.53	1.571051	
6	s_{11}	0.025	0.068074	0.38	0.067705	6
	s_{12}	-0.075	-0.025868	2.9	-0.025259	
	s_{22}	30.250	0.918270	0.23	0.917768	
	s_{66}	5.500	1.560100	3.53	1.555874	

Table 5: Identified parameters $(s_{11},s_{12},s_{22},s_{66})$ of Case 1 by considering different δ.

noise	Parameters ($\times10^{-10}$Pa^{-1})	Initial values	True values	Identified	Relative error	Iterations
3%	s_{11}	0.0150	0.068074	0.068010	0.093%	7
	s_{12}	-0.008	-0.025868	-0.027165	5.012%	
	s_{22}	3.000	0.918270	0.903201	1.641%	
	s_{66}	5.500	1.560100	1.590377	1.941%	
5%	s_{11}	0.0150	0.068074	0.069884	2.659%	9
	s_{12}	-0.008	-0.025868	-0.027135	4.899%	
	s_{22}	3.000	0.918270	0.907567	1.165%	
	s_{66}	5.500	1.560100	1.574977	0.954%	
7%	s_{11}	0.0150	0.068074	0.070249	3.194%	9
	s_{12}	-0.008	-0.025868	-0.026514	2.496%	
	s_{22}	3.000	0.918270	0.927833	1.041%	
	s_{66}	5.500	1.560100	1.592900	2.102%	

that for more complex shaped domains, it is necessary to deliberately choose the initial values and suitable measured locations to achieve good results.

5 Conclusions

In this study, an inverse method has been established by a combination of the singular boundary method and the Levenberg-Marquardt method to determine material parame-

https://doi.org/10.4208/aamm.2015.m904 Published online by Cambridge University Press

Table 6: Identified parameters (s_{11},s_{12},s_{22}) of the multiply connected plate.

Cases	Parameters ($\times 10^{-10}$Pa^{-1})	Initial values	True values	Initial/Trie	Identified	Iterations
1	s_{11}	0.015	0.068074	0.22	0.067765	7
	s_{12}	-0.010	-0.025868	0.39	-0.025889	
	s_{22}	0.250	0.918270	0.27	0.918545	
2	s_{11}	0.015	0.068074	0.22	0.068037	11
	s_{12}	-0.100	-0.025868	0.39	-0.026278	
	s_{22}	3.500	0.918270	3.81	0.918481	
3	s_{11}	0.350	0.068074	5.14	0.067879	16
	s_{12}	-0.080	-0.025868	3.09	-0.025960	
	s_{22}	3.500	0.918270	3.81	0.918383	
4	s_{11}	0.350	0.068074	5.14	0.068026	13
	s_{12}	-0.080	-0.025868	3.09	-0.025941	
	s_{22}	0.250	0.918270	0.27	0.918138	

ters of two-dimensional orthotropic medium. Thanks to the boundary-only discretization and semi-analytical nature of the SBM, the strategy is found through numerical experiments to be a competitive alternative scheme for the solution of inverse problems.

Three numerical examples are studied to illustrate the validity and stability of the proposed methodology. The results show that the parameters can be identified within only a few iterations by the proposed methodology, provided that the initial guess and the lower and the upper bounds are properly chosen in advance. The Levenberg-Marquardt method is more efficient than the Quasi Newton method and pattern search method. Furthermore, the proposed method is robust to the noisy measurement data, which is inevitable in laboratory tests. The proposed method could identify the material parameters with the relative noise level up to 7%. Nevertheless, more iterations are required to achieve the stopping criteria as the relative noise level increases. In a word, it is promising to extend the present scheme to identification of the elastic constants of orthotropic materials and other materials, such as functionally graded materials and multilayer materials. What's more, the attempts on parameters identification in elastoplastic and elastodynamics would be considered in further research.

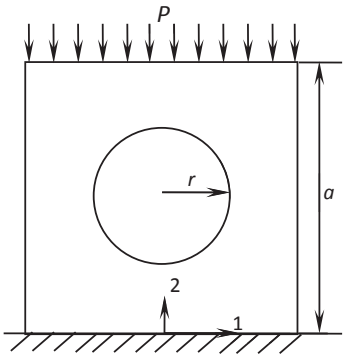


Figure 7: A multiply connected plate.

https://doi.org/10.4208/aamm.2015.m904 Published online by Cambridge University Press

Acknowledgements

The work described in this paper was supported by the National Science Funds for Distinguished Young Scholars of China (Grant No. 11125208), the National Science Funds of China (Grant Nos. 11372097, 11302069), the Fundamental Research Funds for the Central Universities (Grant No. 2013B32814) and the Program of Introducing Talents of Discipline to Universities (111 project, Grant No. B12032).

References

[1] M. R. Hematiyan, A. Khosravifard, Y. C. Shiah and C. L. Tan, *Identification of material parameters of two-dimensional anisotropic bodies using an inverse multi-loading boundary element technique,* CMES-Comput. Model. Eng., 87 (2012), pp. 55–76.
[2] M. Meuwissen, An Inverse Method for the Mechanical Characterization of Metals, Eindhoven University of Technology, 1998.
[3] L. X. Huang, X. S. Sun, Y. H. Liu and Z. Z. Cen, *Parameter identification for two-dimensional orthotropic material bodies by the boundary element method,* Eng. Anal. Bound. Elem., 28 (2004), pp. 109–121.
[4] D. Lecompte, A. Smits, H. Sol, J. Vantomme and D. Van Hemelrijck, *Mixed numericalCexperimental technique for orthotropic parameter identification using biaxial tensile tests on cruciform specimens,* Int. J. Solids. Struct., 44 (2007), pp. 1643–1656.
[5] H. Sol, H. Hua, J. De Visscher, J. Vantomme and W. De Wilde, *A mixed numerical/experimental technique for the nondestructive identification of the stiffness properties of fibre reinforced composite materials,* NDT. E. Int., 30 (1997), pp. 85–91.
[6] W. P. De Wilde, *Identification of the rigidities of composite systems by mixed numerical/experimental methods,* Mechanical Identification of Composites, Springer, 1991, pp. 1–15.
[7] R. Rikards, A. Chate and G. Gailis, *Identification of elastic properties of laminates based on experiment design,* Int. J. Solids. Struct., 38 (2001), pp. 5097–5115.
[8] W. T. Wang and T. Y. Kam, *Material characterization of laminated composite plates via static testing,* Comput. Struct., 50 (2000), pp. 347–352.
[9] M. Grédiac, *The use of full-field measurement methods in composite material characterization: interest and limitations,* Compos. Part A Appl. S., 35 (2004), pp. 751–761.
[10] G. Geymonat and S. Pagano, *Identification of mechanical properties by displacement field measurement: a variational approach,* Meccanica., 38 (2003), pp. 535–545.
[11] F. Eric and L. Gilles, *Using constitutive equation gap method for identification of elastic material parameters: technical insights and illustrations,* IJIDeM., 5 (2011), pp. 227–234.
[12] M. H. H. Meuwissen, C. W. J. Oomens, F. P. T. Baaijens, R. Petterson and J. D. Janssen, *Determination of the elasto-plastic properties of aluminium using a mixed numerical-experimental method,* J. Mater. Process. Tech., 75 (1998), pp. 204–211.
[13] L. Le Magorou, F. Bos and F. Rouger, *Identification of constitutive laws for wood-based panels by means of an inverse method,* Compos. Sci. Technol., 62 (2002), pp. 591–596.
[14] S. S. Chen, Q. H. Li, Y. H. Liu and H. T. Chen, *Identification of elastic orthotropic material parameters by the scaled boundary finite element method,* Eng. Anal. Bound. Elem., 37 (2013), pp. 781–787.
[15] K. T. Kavanagh and R. W. Clough, *Finite element applications in the characterization of elastic solids*, Int. J. Solids. Struct., 7 (1971), pp. 11–23.

https://doi.org/10.4208/aamm.2015.m904 Published online by Cambridge University Press

[16] M. GRÉDIAC, E. TOUSSAINT AND F. PIERRON, *Special virtual fields for the direct determination of material parameters with the virtual fields method. 1–Principle and definition*, Int. J. Solids. Struct., 39 (2002), pp. 2691–2705.
[17] M. GRÉDIAC, E. TOUSSAINT AND F. PIERRON, *Special virtual fields for the direct determination of material parameters with the virtual fields method. 2–Application to in-plane properties,* Int. J. Solids. Struct., 39 (2002), pp. 2707–2730.
[18] M. GRÉDIAC, E. TOUSSAINT AND F. PIERRON, *Special virtual fields for the direct determination of material parameters with the virtual fields method. 3–Application to the bending rigidities of anisotropic plates,* Int. J. Solids. Struct., 40 (2003), pp. 2401–2419.
[19] F. PIERRON, S. ZHAVORONOK AND M. GRÉDIAC, *Identification of the through-thickness properties of thick laminated tubes using the virtual fields method,* Int. J. Solids. Struct., 37 (2000), pp. 4437–4453.
[20] T. OHKAMI, Y. ICHIKAWA AND T. KAWAMOTO, *A boundary element method for identifying orthotropic material parameters,* Int. J. Numer. Anal. Met., 15 (1991), pp. 609–625.
[21] L. X. HUANG, Z. H. XIANG, X. S. SUN, Y. H. LIU AND Z. Z. CEN, *A study of the optimal measurement placement for parameter identification of orthotropic composites by the boundary element method,* Comput. Mech., 38 (2006), pp. 201–209.
[22] X. SUN, L. HUANG, Y. LIU AND Z. CEN, *Boundary element analysis for elastic and elastoplastic problems of 2D orthotropic media with stress concentration,* Acta. Mech. Sinica., 21 (2005), pp. 472–484.
[23] I. MASARU, *Inversion Formulas for the linearized problem for an inverse boundary value problem in elastic prospection,* Soc. Ind. Appl. Math., 50 (1990), pp. 1635–1644.
[24] C. DAMIEN, H. FRANÇOIS AND R. STÉPHANE, *Identification of damage fields using kinematic measurements,* Comptes Rendus Mécanique, 330 (2002), pp. 729–734.
[25] C. DAMIEN, H. FRANÇOIS AND R. STÉPHANE, *Identification of a damage law by using full-field displacement measurements,* Int. J. Damage. Mech., 16 (2007), pp. 179–197.
[26] C. FIORALBA, D. C. MICHELE AND J. G. SUN, *A multistep reciprocity gap functional method for the inverse problem in a multilayered medium,* Complex. Var. Elliptic., 57 (2012), pp. 261–276.
[27] S. AVRIL, M. BONNET, A.-S. BRETELLE, M. GRÉDIAC, F. HILD, P. IENNY, F. LATOURTE, D. LEMOSSE, S. PAGANO, E. PAGNACCO AND F. PIERRON, *Overview of identification methods of mechanical parameters based on full-field measurements,* Exp. Mech., 48 (2008), pp. 381–402.
[28] S. AVRIL AND F. PIERRON, *General framework for the identification of constitutive parameters from full-field measurements in linear elasticity,* Int. J. Solids. Struct., 44 (2007), pp. 4978–5002.
[29] M. A. GOLBERG AND C. S. CHEN, *The method of fundamental solutions for potential, Helmholtz and diffusion problems,* Bound. Integr. Meth. Numer. Math. Aspects., (1998), pp. 103–176.
[30] X. WEI, W. CHEN AND B. CHEN, *An ACA accelerated MFS for potential problems,* Eng. Anal. Bound. Elem., 41 (2014), pp. 90–97.
[31] W. CHEN, *Singular boundary method: a novel, simple, meshfree, boundary collocation numerical method*, Chinese. J. Solid. Mech., 30 (2009), pp. 592–599.
[32] Y. GU, W. CHEN AND C. Z. ZHANG, *Singular boundary method for solving plane strain elastostatic problems,* Int. J. Solids. Struct., 48 (2011), pp. 2549–2556.
[33] Y. GU, W. CHEN AND C. ZHANG, *Stress analysis for thin multilayered coating systems using a sinh transformed boundary element method,* Int. J. Solids. Struct., 50 (2013), pp. 3460–3471.
[34] X. WEI, W. CHEN AND Z. J. FU, *Solving inhomogeneous problems by singular boundary method*, J. Marine Sci. Tech., 21 (2013), pp. 8–14.
[35] Y. GU, W. CHEN, Z.-J. FU AND B. ZHANG, *The singular boundary method: Mathematical background and application in orthotropic elastic problems,* Eng. Anal. Bound. Elem., 44 (2014), pp.

https://doi.org/10.4208/aamm.2015.m904 Published online by Cambridge University Press

152–160.
[36] X. WEI, W. CHEN, B. CHEN AND L. L. SUN, *Singular boundary method for heat conduction problems with certain spatially varying conductivity,* Comput. Math. Appl., 69 (2015), pp. 206–222.
[37] X. WEI, W. CHEN, L. L. SUN AND B. CHEN, *A simple accurate formula evaluating origin intensity factor in singular boundary method for two-dimensional potential problems with Dirichlet boundary,* Eng. Anal. Bound. Elem., 58 (2015), pp. 151–165.
[38] F. J. RIZZO AND D. J. SHIPPY, *A method for stress determination in plane anisotropic elastic bodies,* J. Compos. Mater., 4 (1970), pp. 36–61.
[39] J. J. MORÉ, The Levenberg-Marquardt Algorithm: Implementation and Theory, in: Numerical Analysis, Springer, 1978, pp. 105–116.
[40] W. Y. SUN AND Y. X. YUAN, Optimization Theory and Methods: Nonlinear Programming, Springer, 2006.
[41] J. RHEE AND R. E. ROWLANDS, *Stresses around extremely large or interacting multiple holes in orthotropic composites,* Comput. Struct., 61 (1996), pp. 935–950.
[42] D. F. SHANNO, *Conditioning of quasi-Newton methods for function minimization,* Math. Comput., 24 (1970), pp. 647–656.
[43] A. R. CONN, N. GOULD AND P. L. TOINT, *A globally convergent Lagrangian barrier algorithm for optimization with general inequality constraints and simple bounds,* Math. Comput. Am. Math. Soc., 66 (1997), pp. 261–288.

https://doi.org/10.4208/aamm.2015.m904 Published online by Cambridge University Press